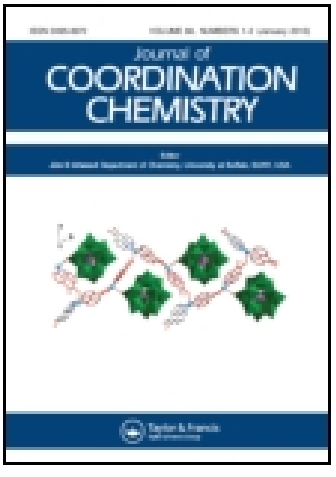

Journal of Coordination Chemistry
Publication details, including instructions for authors and subscription information:
http://www.tandfonline.com/loi/gcoo20

Platinum(II) and palladium(II) aryl-thiosemicarbazone complexes: synthesis, characterization, molecular modeling, cytotoxicity, and antimicrobial activity

T.T. Tavares[a], D. Paschoal[a], E.V.S. Motta[b], A.G. Carpanez[a], M.T.P. Lopes[c], E.S. Fontes[b], H.F. Dos Santos[a], H. Silva[a], R.M. Grazul[a] & A.P.S. Fontes[a]

[a] Departamento de Química, Universidade Federal de Juiz de Fora, Juiz de Fora, Brazil

[b] Departamento de Bioquímica, Universidade Federal de Juiz de Fora, Juiz de Fora, Brazil

[c] Departamento de Farmacologia, Universidade Federal de Minas Gerais, Belo Horizonte, Brazil

Accepted author version posted online: 05 Mar 2014.Published online: 01 Apr 2014.

To cite this article: T.T. Tavares, D. Paschoal, E.V.S. Motta, A.G. Carpanez, M.T.P. Lopes, E.S. Fontes, H.F. Dos Santos, H. Silva, R.M. Grazul & A.P.S. Fontes (2014) Platinum(II) and palladium(II) aryl-thiosemicarbazone complexes: synthesis, characterization, molecular modeling, cytotoxicity, and antimicrobial activity, Journal of Coordination Chemistry, 67:6, 956-968, DOI: 10.1080/00958972.2014.900664

To link to this article: http://dx.doi.org/10.1080/00958972.2014.900664

Journal of Coordination Chemistry, 2014
Vol. 67, No. 6, 956–968, http://dx.doi.org/10.1080/00958972.2014.900664

Platinum(II) and palladium(II) aryl-thiosemicarbazone complexes: synthesis, characterization, molecular modeling, cytotoxicity, and antimicrobial activity

T.T. TAVARES†, D. PASCHOAL†, E.V.S. MOTTA‡, A.G. CARPANEZ†, M.T.P. LOPES§, E.S. FONTES‡, H.F. DOS SANTOS†, H. SILVA†, R.M. GRAZUL† and A.P.S. FONTES*†

†Departamento de Química, Universidade Federal de Juiz de Fora, Juiz de Fora, Brazil
‡Departamento de Bioquímica, Universidade Federal de Juiz de Fora, Juiz de Fora, Brazil
§Departamento de Farmacologia, Universidade Federal de Minas Gerais, Belo Horizonte, Brazil

(*Received 19 September 2013; accepted 1 February 2014*)

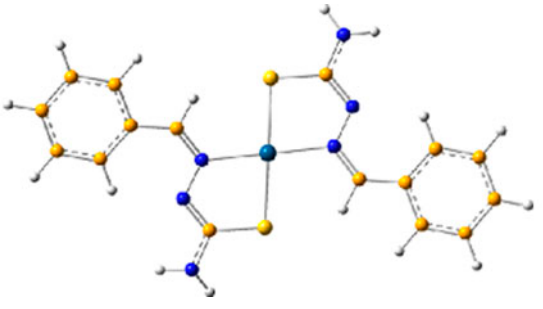

Platinum(II) and palladium(II) complexes [ML_2] have been isolated from reaction of K_2PtCl_4 or K_2PdCl_4 and ligands (L) derived from thiosemicarbazones. The complexes were characterized by elemental analysis, Raman, IR, and NMR spectroscopy. In addition, quantum mechanical calculations were used to predict their structures and spectroscopic properties. For the first time, theoretical calculations using ^{195}Pt NMR data were used to support the suggested structures. The results indicate that the thionic sulfur and the azomethine nitrogen are bonded to the metal ion in a *trans* configuration. Antibacterial activities and cytotoxicities of the complexes to B16-F10 and CT26.WT cell lines were also investigated. Some of the complexes demonstrated superior cytotoxic activity compared to cisplatin.

Keywords: Thiosemicarbazones; Pt(II) and Pd(II) complexes; Cytotoxicity; Molecular modeling

1. Introduction

The majority of potential antitumor metal complexes are structural analogs of cisplatin. However, due to severe side effects and other undesirable properties [1, 2], there has been a

*Corresponding author. Email: ana.fontes@ufjf.edu.br

decrease in the number of compounds based on the cisplatin structure. This has motivated the search for complexes presenting novel structures and promising activity, mainly those with the ability to overcome cisplatin resistance [3].

Metal coordination to biologically active molecules can be used as a strategy to enhance activity and overcome resistance. For instance, metal complexes of thiosemicarbazones are often more active than the free ligand, or even act as a vehicle for activation of the ligand as the cytotoxic agent [2, 3]. The coordination chemistry of thiosemicarbazones has generated interest for their variable donor ability, structural diversity, and biological applications [4, 5]. Thiosemicarbazones are among the most potent inhibitors of ribonucleotide reductase activity. This enzyme catalyzes the synthesis of DNA and is responsible for maintaining the balanced supply of deoxyribonucleotides required for DNA synthesis and repair. Strong positive correlation has been established between ribonucleotide reductase activity and antitumor activity [6]. Platinum(II) and palladium(II) complexes with thiosemicarbazones are particularly attractive because of their antitumor [7], antibacterial [8], antiviral [9], and cytotoxic activities [10, 11].

The combination of thiosemicarbazones with platinum(II) and palladium(II) can also produce synergistic inhibition of tumor growth and may lead to improvements in the efficacy of cancer chemotherapy [4, 12, 13]. Palladium complexes with thiosemicarbazones show antitumor activities and some are also active in cell lines resistant to cisplatin, presenting decreased nephrotoxicity [14, 15].

Thiosemicarbazones may incorporate heterocyclic or aromatic rings. Due to their biological activities, such molecules have attracted interest. They have been previously described to present nematocidal, insecticidal, antibacterial, antifungal, antiviral, and anti-inflammatory activities, especially for furan and thiophene side groups [16].

The coordination chemistry of metal complexes with thiosemicarbazones has been intensively investigated. Usually they bind to a metal ion via dissociation of the hydrazine proton, as a bidentate N, S donor, forming a five-membered chelate ring [17]. The ligands may feature more than two binding sites, depending on the precursor aldehyde, and on the tautomeric equilibrium of the thiosemicarbazone.

As part of our continuing investigations on metal complexes as anticancer [18, 19] and antimicrobial [20, 21] agents, we report herein the synthesis, characterization, and cytotoxic/antimicrobial activity of palladium(II) and platinum(II) complexes containing thiosemicarbazone ligands. The compounds were characterized by Raman, IR, and NMR (^{1}H, ^{13}C, ^{195}Pt) spectroscopy and elemental analysis, in addition to quantum mechanical calculations.

2. Experimental

2.1. *Materials and methods*

All reagents and solvents were used as obtained from commercial sources (Aldrich Sigma) without purification. The thiosemicarbazones were prepared according to previously reported methods [22].

Melting points were determined with a MQAPF-Microquímica hot-stage apparatus. Elemental analyses were performed at the University of São Paulo, Brazil. IR spectra were obtained on a Bomem FT IR MB-102 spectrometer as KBr pellets. Fourier-transform Raman spectroscopy was carried out using a Bruker RFS 100 instrument equipped with an

Nd^{3+}/YAG laser operating at 1064 nm in the near infrared with a CCD detector cooled with liquid nitrogen with an average of 1000 scans and a spectral resolution of 4 cm^{-1}. ^{1}H NMR (300 MHz), ^{13}C NMR (75 MHz), and ^{195}Pt NMR (64 MHz) spectra were recorded on a Bruker spectrometer by dissolving the complexes in DMSO-d_6. The chemical shifts are expressed as δ (in ppm) from internal reference standards, TMS (^{1}H and ^{13}C NMR) and K_2PtCl_6 (^{195}Pt NMR). Mass spectra were obtained on an AXIMA MALDI-TOF-TOF Shimadzu Biotech equipment. A nitrogen laser ($\lambda_{max} = 337$ nm) was employed for excitation in a α cyano matrix. 200 scans were accumulated with 20 repetitions each.

2.2. *Synthesis of ligands*

The thiosemicarbazone ligands were prepared according to the literature procedure [22] (scheme 1). To a hot solution of thiosemicarbazide (31.25 mM) in 50 mL of methanol, a solution of the corresponding aromatic aldehyde (31.25 mM) in 30 mL of methanol was added dropwise. The mixture was stirred and refluxed for 4 h, cooled, and then filtered. The volume of the filtrate was reduced and kept in a refrigerator. After several hours, yellow or white solids were obtained, isolated by filtration, washed with cold ethanol, and dried under vacuum. (**a**) ($C_8H_9N_3S$), white solid, yield = 62%, m.p. 158–160 °C; (**b**) ($C_9H_{11}ON_3S$), white solid, yield = 82%, m.p. 174–175 °C; (**c**) ($C_6H_7N_3S_2$), pale yellow solid, yield = 74%, m.p. 189–190 °C; (**d**) ($C_6H_7ON_3S$), pale yellow solid, yield = 61%, m.p. 152–153 °C; (**e**) ($C_7H_8N_4S$), beige solid, yield = 88%, m.p. 217–219 °C; (**f**) ($C_8H_9ON_3S$), beige solid, yield = 65%, m.p. 237–238 °C.

2.3. *Synthesis of complexes*

A suspension of potassium tetrachoroplatinate or potassium tetrachloropalladate (0.5 mM) in methanol (10 mL) was added with stirring to a solution of the corresponding ligand (1 mM) in methanol (10 mL) containing triethylamine (2 mM; scheme 2). The solution was refluxed for 24 h for the palladium complexes. For the platinum complexes, reflux was maintained between 10 and 20 days. The complete consumption of the starting material was evidenced by thin-layer chromatography (TLC; eluent: 9:1 dichloromethane/methanol). The precipitate thus formed was collected by filtration and dried in vacuum. Yields: (**1**) 74%, (**2**) 42%, (**3**) 64%, (**4**) 61%, (**5**) 67%, (**6**) 31%, (**7**) 40%, (**8**) 79%, (**9**) 70%, (**10**) 87%, (**11**) 61%, (**12**) 66%.

(**1**) IR ν_{max} KBr (cm^{-1}): 3420, 3274, 1598, 1586, 1025, 847; Raman (cm^{-1}): 1578, 1556, 1180, 872, 433, 400. ^{1}H NMR (300 MHz, DMSO-d_6) δ: 7.79 m, 2H, NH_2); 7.78,7.44 (m, 6H, Ph), 8.14 (s, 1H, *H*C=N); ^{13}C NMR (75 MHz, DMSO-d_6) δ: 132.38, 132.32, 130.70, 128.29, 128.10 and 11.32 (C, Ph); 143.36 (H*C*=N); 176.16 (*C*-S); ^{195}Pt NMR (64 MHz, DMSO-d_6) δ: –3126. Anal. Calcd for $C_{16}H_{16}N_6S_2Pt$ (%): C, 34.85; H, 2.90; N, 15.25. Found: C, 34.72; H, 3.02; N, 14.71. MS (MALDI): *m*/*z* Calcd for $[C_{16}H_{17}N_6S_2Pt]$ $[M + H]^+$ Calcd (552.1) found 552.5.

(**2**) IR ν_{max} KBr (cm^{-1}): 3468, 3359, 1603, 1563, 1012, 856; Raman (cm^{-1}): 1585, 1537, 1165, 869, 486, 400. ^{1}H NMR (300 MHz, DMSO-d_6) δ: 3.83 (s, 3H, CH_3); 7.33 (s, 2H, NH_2); 8.18, 8.15, 6.99, 6.96 (dd, 6H, Ph), 7.72 (s, 1H, *H*C=N); ^{13}C NMR (75 MHz, DMSO-d_6) δ: 160.91, 134.59, 125.43 and 113.49 (C, Ph); 154.16 (H*C*=N); 175.08 (*C*–S); ^{195}Pt NMR (64 MHz, DMSO-d_6) δ: −3143. Anal. Calcd for $C_{18}H_{20}N_6S_2O_2Pt$ (%): C, 35.35; H, 3.27; N, 13.03. Found: C, 35.31; H, 3.50; N, 13.75. MS (MALDI): *m*/*z* Calcd for $[C_{18}H_{21}N_6S_2O_2Pt]$ $[M + H]^+$ Calcd (612.1) found 612.2.

(**3**) IR ν_{max} KBr (cm^{-1}): 3461, 3358, 1599, 1572, 1062, 813. Raman (cm^{-1}): 1578, 1522, 1083, 857, 456, 388. ^{1}H NMR (300 MHz, DMSO-d_6) δ: 7.34 (s, 2H, N*H*$_2$); 8.07, 7.94, 7.64, 7.15 (dd, 4H, Ph), 8.11 (s, 1H, *H*C=N); ^{13}C NMR (75 MHz, DMSO-d_6) δ: 149.42, 141.89, 140.34, 132.44 (C, Ph); 153.01 (H*C*=N); 182.04 (*C*-S); ^{195}Pt NMR (64 MHz, DMSO-d_6) δ: −3012. Anal. Calcd for $C_{12}H_{12}N_6S_4Pt$ (%): C, 25.58; H, 2.13; N, 14.92. Found: C, 25.79; H, 2.18; N, 14.15. MS (MALDI): *m*/*z* Calcd for $[C_{12}H_{13}N_6S_4Pt]$ $[M+H]^+$ Calcd (564.0) found 564.5.

(**4**) IR ν_{max} KBr (cm^{-1}): 3405, 3295, 1608, 1588, 1091, 862. Raman (cm^{-1}): 1590, 1503, 1146, 823, 452, 418. ^{1}H NMR (300 MHz, DMSO-d_6) δ: 7.56 (s, 2H, N*H*$_2$); 7.77, 7.76, 7.70, 6.75 (dd, 4H, Ph), 7.90 (s, 1H, *H*C=N); ^{13}C NMR (75 MHz, DMSO-d_6) δ: 146.07, 141.76, 121.54, 121.54 and 113.03 (C, Ph); 147.69 (H*C*=N); 175.79 (*C*-S); ^{195}Pt NMR (64 MHz, DMSO-d_6) δ: −2999. Anal. Calcd for $C_{12}H_{12}N_6S_2O_2Pt$ (%): C, 27.12; H, 2.26; N, 15.49. Found: C, 27.16; H, 2.42; N, 15.82. MS (MALDI): *m*/*z* Calcd for $[C_{12}H_{13}N_6S_2O_2Pt]$ $[M+H]^+$ Calcd (532.0) found 532.3.

(**5**) IR ν_{max} KBr (cm^{-1}): 3417, 3288, 1632, 1589, 1040, 859. Raman (cm^{-1}): 1593, 1541, 1154, 850, 418, 384. ^{1}H NMR (300 MHz, DMSO-d_6) δ: 7.07 (s, 2H, N*H*$_2$); 8.69, 8.36, 7.85, 7.68, 7.61, 7.38 (m, 5H, Ph), 8.08 (s, 1H, *H*C=N); ^{13}C NMR (75 MHz, DMSO-d_6) δ: 151.96, 138.49, 125.19 (C, Ph); 150.11 (H*C*=N); 178.19 (*C*-S); ^{195}Pt NMR (64 MHz, DMSO-d_6) δ: −2932. Anal. Calcd for $C_{14}H_{14}N_8S_2Pt$ (%): C, 30.38; H, 2.74; N, 20.25. Found: C, 31.31; H, 3.11; N, 22.30. MS (MALDI): *m*/*z* Calcd for $[C_{14}H_{15}N_8S_2Pt]$ $[M+H]^+$ Calcd (554.1) found 554.1.

(**6**) IR ν_{max} KBr (cm^{-1}): 3426, 3321, 1598, 1574, 1025, 827. Raman (cm^{-1}): 1560, 1537, 1169, 869, 414, 384. ^{1}H NMR (300 MHz, DMSO-d_6) δ: 7.22 (s, 2H, N*H*$_2$); 8.06, 8.03, 6.81, 6.78 (m, 6H, Ph), 7.65 (s, 1H, *H*C=N); ^{13}C NMR (75 MHz, DMSO-d_6) δ: 160.13, 135.13, 124.32, 115.22 (C, Ph); 135.16 (H*C*=N); 174.87 (*C*-S); ^{195}Pt NMR (64 MHz, DMSO-d_6) δ: −2931. Anal. Calcd for $C_{16}H_{16}N_6S_2O_2Pt$ (%): C, 32.93; H, 2.74; N, 14.41. Found: C, 31.80; H, 2.55; N, 13.97. MS (MALDI): *m*/*z* Calcd for $[C_{16}H_{17}N_6S_2O_2Pt]$ $[M+H]^+$ Calcd (584.1) found 584.3.

(**7**) IR ν_{max} KBr (cm^{-1}): 3452, 3330, 1615, 1574, 1023, 868. Raman (cm^{-1}): 1596, 1574, 1173, 874, 470, 405. ^{1}H NMR (300 MHz, DMSO-d_6) δ: 7.27 (m, 2H, N*H*$_2$); 7.66, 7.58, 7.37, 6.79 (m, 6H, Ph), 7.37 (s, 1H, *H*C=N); ^{13}C NMR (75 MHz, DMSO-d_6) δ: 132.24, 130.62, 130.03, 127.29 (C, Ph); 155.02 (H*C*=N); 172.81 (*C*–S); Anal. Calcd for $C_{16}H_{16}N_6S_2Pd$ (%): C, 41.52; H, 3.83; N, 18.17. Found: C, 39.92; H, 3.91; N, 17.27. MS (MALDI): *m*/*z* Calcd for $[C_{16}H_{17}N_6S_2Pd]$ $[M+H]^+$ Calcd (463.1) found 463.5.

(**8**) IR ν_{max} KBr (cm^{-1}): 3458, 3336, 1609, 1566, 1018, 827. Raman (cm^{-1}): 1593, 1571, 1173, 880, 422, 396. ^{1}H NMR (300 MHz, DMSO-d_6) δ: 3.79 (s, 3H, C*H*$_3$); 6.66 (s, 2H, N*H*$_2$); 7.56, 7.53, 6.88, 6.85 (dd, 6H, Ph), 7.38 (s, 1H, *H*C=N); ^{13}C NMR (75 MHz, DMSO-d_6) δ: 160.84, 131.46, 124.40, 112.24 (C, Ph); 154.76 (H*C*=N); 171.48 (*C*–S). Anal. Calcd for $C_{18}H_{20}N_6S_2O_2Pd.CH_3OH$ (%): C, 41.12; H, 4.32; N, 15.15. Found: C, 40.08; H, 4.16; N, 15.12. MS (MALDI): *m*/*z* Calcd for $[C_{18}H_{21}N_6S_2O_2Pd]$ $[M+H]^+$ Calcd (523.0) found 523.3.

(**9**) IR ν_{max} KBr (cm^{-1}): 3443, 3281, 1598, 1572, 1057, 825. Raman (cm^{-1}): 1578, 1576, 1146, 857, 418, 317. ^{1}H NMR (300 MHz, DMSO-d_6) δ: 7.13 (s, 2H, N*H*$_2$); 7.87, 7.86, 7.11, 7.10 (dd, 4H, Ph), 7.58 (s, 1H, *H*C=N); ^{13}C NMR (75 MHz, DMSO-d_6) δ: 135.58, 133.95, 132.89, 126.56 (C, Ph); 146.78 (H*C*=N); 173.07 (*C*–S). Anal. Calcd for $C_{12}H_{12}N_6S_4Pd$ (%): C, 30.35; H, 2.53; N, 17.71. Found: C, 30.32; H, 2.68; N, 17.29. MS (MALDI): *m*/*z* Calcd for $[C_{12}H_{13}N_6S_4Pd]$ $[M+H]^+$ Calcd (474.9) found 475.1.

(**10**) IR ν_{max} KBr (cm^{-1}): 3478, 3303, 1609, 1592, 1082, 889. Raman (cm^{-1}): 1585, 1560, 1150, 828, 425, 381. ^{1}H NMR (300 MHz, DMSO-d_6) δ: 7.34 (s, 2H, N*H*$_2$); 7.62, 7.64, 7.18, 6.70, 6.69 (dd, 4H, Ph), 7.84 (s, 1H, *H*C=N); ^{13}C NMR (75 MHz, DMSO-d_6) δ: 146.09, 140.85, 121.21, 113.32 (C, Ph); 147.17 (H*C*=N); 174.57 (*C*–S). Anal. Calcd for $C_{12}H_{12}N_6S_2O_2Pd$ (%): C, 32.55; H, 2.71; N, 18.99. Found: C, 32.77; H, 2.91; N, 18.90. MS (MALDI): *m/z* Calcd for $[C_{12}H_{13}N_6S_2O_2Pd]$ $[M+H]^+$ Calcd (443.0) found 443.3.

(**11**) IR ν_{max} KBr (cm^{-1}): 3470, 3410, 1619, 1593, 1027, 865. Raman (cm^{-1}): 1593, 1574, 1199, 857, 444, 392. ^{1}H NMR (300 MHz, DMSO-d_6) δ: 7.25 (s, 2H, N*H*$_2$); 8.65, 8.63, 8.19, 7.66, 7.63, 7.55 (m, 5H, Ph), 8.21 (s, 1H, *H*C=N); ^{13}C NMR (75 MHz, DMSO-d_6) δ: 138.31, 137.87, 125.29, 125.09 (C, Ph); 147.27 (H*C*=N); 176.60 (*C*–S). Anal. Calcd for $C_{14}H_{14}N_8S_2Pd$ (%): C, 36.18; H, 3.01; N, 24.12. Found: C, 35.82; H, 2.86; N, 23.15. MS (MALDI): *m/z* Calcd for $[C_{14}H_{15}N_8S_2Pd]$ $[M+H]^+$ Calcd (465.0) found 465.4.

(**12**) IR ν_{max} KBr (cm^{-1}): 3392, 3305, 1600, 1598, 1029, 816. Raman (cm^{-1}): 1588, 1512, 1176, 805, 414, 343. ^{1}H NMR (300 MHz, DMSO-d_6) δ: 6.98 (s, 2H, N*H*$_2$); 7.99, 7.97, 6.97, 6.76 (m, 6H, Ph), 7.14 (s, 1H, *H*C=N); ^{13}C NMR (75 MHz, DMSO-d_6) δ: 160.08, 135.10, 123.85, 115.28 (C, Ph); 153.99 (H*C*=N); 173.36 (*C*–S). Anal. Calcd for $C_{16}H_{16}N_6S_2O_2Pd$ (%): C, 38.83; H, 3.24; N, 16.99. Found: C, 38.06; H, 3.18; N, 16.97. MS (MALDI): *m/z* Calcd for $[C_{16}H_{17}N_6S_2O_2Pd]$ $[M+H]^+$ Calcd (495.0) found 495.3.

2.4. *Cytotoxicity assay*

Cytotoxic activities were investigated against the following tumor cell lines: B16-F10 – mouse metastatic skin melanoma, CT26.WT – colon cancer cells (Ludwig Institute of Cancer Research – São Paulo – Brazil), and the non-tumor cell line BHK-21 – Baby Hamster Kidney (Centro Panamericano de Febre Aftosa – Rio de Janeiro – Brazil). All cell lines were propagated in RPMI 1640 culture medium at pH 7.4, supplemented with 10% heat-inactivated fetal bovine serum (FBS), HEPES (4.0 mM), $NaHCO_3$ (14.0 mM), ampicillin (0.27 mM), and streptomycin (0.06 mM).

Cells were harvested by trypsinization and seeded in 96-well tissue culture plates (100 µL/well) at different densities according to the cell line (0.5×10^3–2×10^3 viable cells/well) and incubated at 37 °C in a humidified atmosphere containing 5% CO_2 for 24 h. Stock solutions of the test substances in DMSO were serially diluted in cell culture medium (<1% DMSO). After drug exposure for 72 h at 37 °C and 5% CO_2, cells were incubated with MTT (0.01 M in water – 10 µL/well) for 4 h at 37 °C and 5% CO_2. MTT is metabolized by viable cells resulting in a violet product that, after being solubilized in 100 µL of DMSO, can be quantified through colorimetric assay using an ELISA reader (absorbance at 570 nm).

The negative control (100% value of viability) was obtained with cells exposed to RPMI 1640 medium supplemented with 10% FBS. Positive controls (cisplatin) were also used against these cell lines.

The raw data were normalized to the untreated control cells and set relative to the metabolic activity of the viable treated cells. IC_{50} values were calculated by four parametric non-linear regression using Graph Pad Prism 5.0 software.

2.5. *Antimicrobial assay*

The samples were evaluated against the bacterial strains *Staphylococcus aureus* (ATCC 29213), *Pseudomonas aeruginosa* (ATCC 27853), *Shigella dysenteriae* (ATCC 13313), *Salmonella enterica* subsp. *enterica serovar typhimurium* (ATCC 13311), *Escherichia coli* (ATCC 10536), and *Enterobacter cloacae* (ATCC 23355).

The MIC of each sample was determined using broth microdilution techniques for bacteria (NCCLS, 2002). MIC values were determined in Mueller-Hinton broth (MHB). Bacterial strains were cultured overnight at 37 °C in Brain Heart Infusion agar. Sample stock solutions were twofold diluted from 200 to 1.56 μg mL^{-1} (final volume = 80 μL) and a final DMSO concentration ≤ 1%. Then, MHB (100 μL) was added onto 24 microplates. Finally, 20 μL of 10^6 CFU/mL (values of 0.08–0.10 at 625 nm, according to McFarland turbidity standards) of standardized bacterial suspensions were inoculated onto microplates and the test was performed with a volume of 200 μL. Plates were incubated at 37 °C for 24 h. The same tests were performed simultaneously for growth control (MHB + bacteria) and sterility control (MHB + extract). The MIC values were calculated as the highest dilution showing complete inhibition of the tested strain. Chloramphenicol (100–0.78 μg mL^{-1}) was used as positive control [23].

2.6. *Calculations*

Quantum mechanical calculations using density functional theory (DFT) were used to predict structures and spectroscopic properties of the Pt(II) and Pd(II)-thiosemicarbazone complexes. The geometries for the *cis* and *trans* isomers were optimized in the gas phase at the B3LYP level [24] with the 6-31+G(d) basis set used for hydrogen and heavy elements, except for the metal for which the LanL2DZ [25] effective core potential was set for core electrons with its balanced double-zeta basis set for valence electrons [26]. This calculation scheme is abbreviated as B3LYP/LanL2DZ/6-31+G(d) and was recently evaluated for cisplatin reactivity [27]. The same level of theory was used for vibrational frequency calculation in order to characterize the structures as true minima on the potential energy surface (all harmonic frequencies real) as well as to analyze the vibrational normal modes. NMR predictions were also accomplished for ^{1}H, ^{13}C, and ^{195}Pt nuclei in order to assist the experimental assignments. The gage-independent atomic orbital method implemented by Wolinski, Hilton and Pulay [28] was used for calculation of magnetic shielding constants (σ) and the chemical shifts (δ), obtained on a δ-scale relative to the TMS (^{1}H and ^{13}C) and K_2PtCl_6 (^{195}Pt). For Pd(II) complexes, with only ^{1}H and ^{13}C nuclei active, the B3LYP/LanL2DZ/6-311++G(2df,2pd)// level of calculation was used with solvent effect (DMSO) included through the IEFPCM continuum model [29]. The double slash signifies that the geometries were those calculated at B3LYP/LanL2DZ/6-31+G(d) level. For Pt(II), in which the ^{195}Pt nuclei is also active, a distinct methodology was applied. The B3LYP level was used accounting for Douglas–Kroll–Hess (DKH) fourth-order relativistic calculations including spin-orbit terms [30]. The basis set for all atoms was the NMR-TZPP-DKH, which was specifically constructed for ^{195}Pt NMR prediction [31]. This calculation scheme is abbreviated as B3LYP-DHKSO/NMR-TZPP-DKH//. All calculations were carried out using the Gaussian 09 suite of programs [32].

3. Results and discussion

3.1. *Structures and spectroscopic characterization*

The thiosemicarbazones used as ligands were prepared by the classical method that consists of condensation of the aldehyde and thiosemicarbazide [22]. They were characterized using IR, ^{1}H, and ^{13}C NMR and by comparison with the data reported in the literature [33, 34].

Structures for Pd(II) and Pt(II) complexes with benzaldehyde thiosemicarbazone have been described by Hernández and collaborators [35]. They found that Pd forms a bis-chelated complex whereas the Pt complex is tetranuclear. To the best of our knowledge, the other complexes are new, although different structures with the same ligands have been described. For example, Lobana and coworkers [36] have described a palladium complex with triphenylphosphine- and thiophene thiosemicarbazone-coordinated tridentate through the N, S, and C. Antelo *et al.* [37] reported the study of palladium and platinum bimetallic compounds with *p*-hydroxyphenyl thiosemicarbazone.

We were not able to obtain crystals for X-ray diffraction, therefore definitive solid-state structures could not be obtained. Nonetheless, gas-phase geometries were predicted with the aid of DFT calculations. The metal : ligand 1 : 2 stoichiometry was observed from elemental analysis with the thiosemicarbazone in the *Z* form. The *cis* and *trans* forms are presented in figure 1 (for the benzene analog) with the main structural data quoted in table S1 and given as Supplementary materials (see online supplemental material at http://dx.doi.org/10.1080/00958972.2014.900664). The *trans* isomer was more stable than the *cis* isomer, regardless of the ligand derivative, with Gibbs free energy difference ~3 kcal M^{-1} (Pt complexes) and ~1 kcal M^{-1} (Pd complexes). The kinetics for formation of *cis* and *trans* isomers also favors the *trans* form. Using a simpler model with R=CH_3 in scheme 2, the free-energy barrier was 4 kcal M^{-1} lower for the reaction leading to the *trans* isomer than the corresponding process for the *cis* complex in methanol solution at 298.15 K. Therefore, the theoretical analysis presented here is focused on the *trans* isomer with some data for the *cis* form given as comparison. The *trans* complexes were planar with a slightly distorted square-planar geometry around the metal. The M–N and M–S bond lengths (M=Pt or Pd) were predicted as 2.07 and 2.37 Å, respectively, and the S–M–N angle was predicted to be 82° (see table S1). These values are in agreement with X-ray data reported for the Pd(II) complex of *m*-cyanobenzaldehyde thiosemicarbazone which were found to be 2.05, 2.30 Å, and 82.8°, respectively [35].

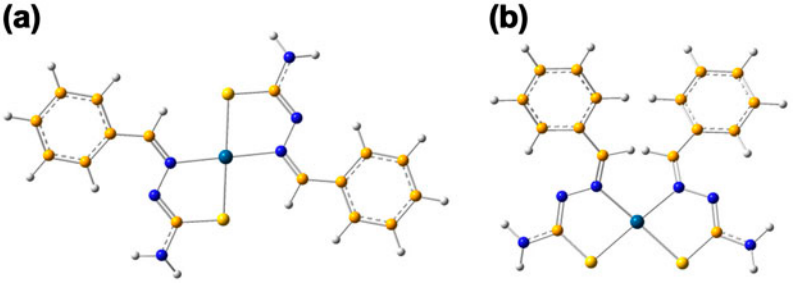

Figure 1. B3LYP/LanL2DZ/6-31+G(d) optimized geometries for *trans* (a) and *cis* (b) forms of **1**.

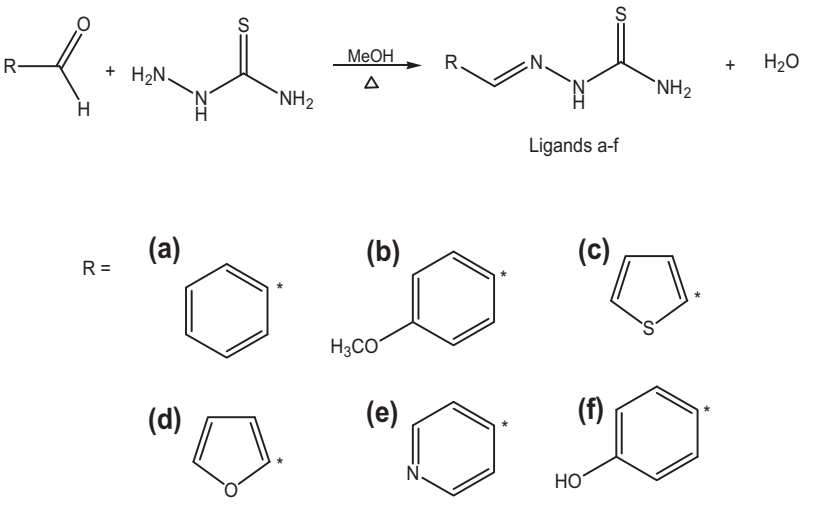

Scheme 1.

The experimental IR spectra of the free ligands showed broad bands at 3145 cm^{-1} assigned to N–H stretch, which disappear in spectra of the complexes indicating deprotonation of the HN-CS. A strong band was observed at 1605 cm^{-1} for the free ligands due to ν(C=N) [38]. Theoretically, two transitions were calculated at 1688 cm^{-1} (ν(C=N) – very weak) and 1666 cm^{-1} ($\delta(NH_2)$ – very strong. Theoretical frequencies in this region are overestimated and it is common to scale those using linear factors. Herein, we preferred to keep values without scaling, as the purpose is to assist the vibrational assignment and not reproduce exactly the vibrational frequencies. Theoretical IR calculations also predicted an intense transition at ~1577 cm^{-1} due to the H–NCS in-plane deformation, which could be

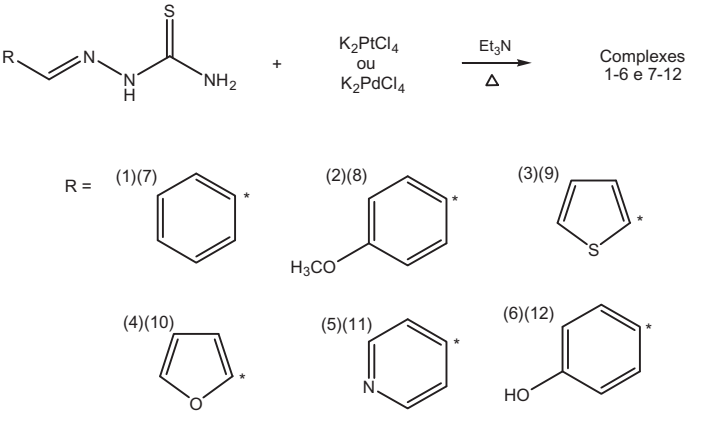

Scheme 2.

useful to follow deprotonation upon complexation. Experimentally, for the complexes, the band at ~1605 cm^{-1} (free ligand) was shifted to lower frequencies (~1578 cm^{-1}) suggesting coordination through the imine nitrogen in a bis-chelate mode [39]. The calculated values for ν(C=N) ranged from 1630 to 1653 cm^{-1}, with the lowest predicted for the pyridine analogs (**5** and **11**) and the highest frequency calculated for the furan derivatives (**4** and **10**). Note that a shift to lower frequencies was observed due to metal coordination to nitrogen. As discussed previously for the free ligand, the $\delta_{ip}(NH_2)$ mode, calculated at ~1665 cm^{-1} for the complexes (the same frequency as the ligand), is more intense than ν(C=N). A very intense transition was calculated at 1544–1571 cm^{-1} assigned to ν(SC–N). Therefore, focusing on the theoretical IR in the 1500–1700 cm^{-1} region, two intense bands were predicted for the free ligand and complexes. For the free ligand, the bands were centered at 1577 cm^{-1} (δ_{ip}(H-NCS)) and 1666 cm^{-1} ($\delta(NH_2)$); while for the complexes, they were found at ~1560 cm^{-1} (ν(SC–N)) and ~1667 cm^{-1} ($\delta_{ip}(NH_2)$). The IR assignment of the first band is distinct for the ligand and complex due to deprotonation upon coordination. The SC–N stretch was calculated at a fairly high frequency due to double-bond character of this bond (see figure 1). The next set of intense IR bands was found around 1340 cm^{-1} and assigned mainly to ν(C-NH_2). For ligands, this same mode was calculated around 1290 cm^{-1}. Experimentally, ν(C=S) was observed as medium bands at 1090–835 cm^{-1} (free ligands) and at lower frequencies (~1025–813) on coordination of the thiocarbonyl sulfur to platinum(II) or palladium(II). The ν(C=S) mode was calculated at ~770 cm^{-1} (free ligands) and ~670 cm^{-1} (complexes) with very low intensity. These IR data are in agreement with those observed for thiosemicarbazone complexes [35]. The calculated vibrational frequencies and assignments are given in table S2 as Supplementary materials.

In Raman spectra, ν(C=N) was predicted to be very intense at 1634 cm^{-1} coupled to ν(C=C) of the aromatic ring. A set of weak bands was observed around 1500 cm^{-1} due to δ_{ip}(CH-Ar) with the most intense transition within this set assigned to δ_{ip}(C–H) at ~1450 cm^{-1}. The stretching mode ν(HC–C) was also active in the Raman spectrum at ~1235 cm^{-1} as well as the ν(N–N) vibration at ~1183 cm^{-1}. Metal–ligand modes were also predicted in Raman at ~535 ν(M–N) and ~317 ν(M–S) with very low intensity. Experimentally these M–L bands were observed around 440 and 380 cm^{-1}, respectively.

The NMR spectra of the thiosemicarbazones and their platinum(II) and palladium(II) complexes were recorded in DMSO-d_6. In the ^{1}H-NMR spectra of the ligands, signals of the =N-N*H* protons were observed as a singlet at δ 11.4. This is indicative of the predominance of the thione form in the *E* configuration [40]. This signal disappeared in ^{1}H NMR spectra of the complexes due to deprotonation of =N–N*H*, which indicates the formation of the complexes. The signal of the *H*C=N protons which appeared as a singlet at δ 8.1 in spectra of the ligands (calculated at δ 10.4) showed an upfield shift after complexation, which indicates coordination of the imine nitrogen to the metal [41]. The calculated values range from δ 7.40–8.10 (Pt complexes) and 6.87–7.53 (Pd complexes), which agree satisfactorily with the experimental data. The signals of the aromatic protons of the complexes were observed at δ 7.1–8.3, and they did not suffer relevant changes compared to the free ligands. The NH_2 signal in the ligands appeared as doublets centered at δ 8.1 due to non-equivalence of the amine protons, attributed to restricted rotation around the C–NH_2 bond (thiocarbonyl carbon and terminal amine nitrogen) due to its partial-double-bond character [42]. In spectra of the complexes, this signal was observed at δ 7.5.

In ^{13}C NMR spectra of the complexes, the signals of the HC=N group occur at δ 154. The C=S signal, observed at δ 173, is characteristic of this group [43], while the aromatic carbons were observed in the δ 154–114 region. The calculated values for HC=N and C=S

were slightly overestimated (~5%), the average chemical shifts found at 160 and 185 ppm, respectively.

Theoretical calculations concerning the predicted ^{195}Pt NMR spectra were used for the first time [31]. In ^{195}Pt NMR spectra of the complexes, a signal around δ –3000 was observed, expected for coordination of platinum to two sulfurs and two nitrogens [44]. The calculated values were obtained for both the *cis* and *trans* complexes in order to support the predominance of the *trans* isomer. The agreement with experimental results was much better for the *trans* structure, with an average absolute deviation of approximately 283 ppm (~10%), whereas for the *cis* isomer, it was 622 ppm (~20%). According to our previous study [31], where the methodology was developed and tested for ^{195}Pt NMR prediction, the average deviation was ~60 ppm, with maximum error for a set of 27 molecules equal to 150 ppm. The shift predicted for *cis* and *trans* signals in the present study (~300 ppm) is higher than our confidence limit, therefore, the level of theory applied here might be satisfactory to distinguish between isomeric forms.

3.2. *Cytotoxic activity*

The cytotoxicities of the complexes were evaluated in comparison with cisplatin in two tumor cell lines: colon cancer cells (CT26.WT) and melanoma (B16-F10). The complexes were also examined for their cytotoxic properties on one normal, i.e., non-tumor kidney cell line (BHK-21). The tumor cells were chosen to represent two different tumor types, melanoma and carcinoma, and to also assess the activity in cell lines of different embryonic origin such as epithelial and fibroblast. This was done in an effort to overcome and control any differences. The third cell line is a normal cell, which was used to evaluate the selectivity index, allowing comparison of the cytotoxicity of the compounds in tumor and normal cells.

Table 1. Cytotoxic activities against tumor cell lines (B16-F10 and CT26.WT) and non-tumor cell lines (BHK). IC_{50} (μM ± SD)*.

Compound	B16-F10 (μM ± SD)*	SI**	CT26.WT (μM ± SD)*	SI**	BHK-21 (μM ± SD)*
Ligand **a**	>100	NA	2.2 ± 2.1	NA	>100
Ligand **b**	>100	NA	2.7 ± 1.7	19.6	53.1 ± 4.1
Ligand **c**	>100	NA	1.0 ± 0.7	66.3	66.3 ± 1.3
Ligand **d**	>100	NA	2.6 ± 2.7	NA	>100
Ligand **e**	>100	NA	8.6 ± 0.4	NA	>100
Ligand **f**	>100	NA	1.6 ± 0.7	NA	>100
Complex **1**	3.6 ± 0.6	4.3	4.4 ± 3.4	3.5	15.5 ± 2.9
Complex **2**	0.4 ± 0.3	83.7	<0.1	335.0	33.5 ± 2.1
Complex **3**	12.3 ± 3.7	4.1	9.6 ± 0.4	5.3	50.9 ± 14.9
Complex **4**	0.4 ± 0.3	151.0	0.6 ± 0.4	100.7	60.4 ± 3.2
Complex **5**	11.4 ± 1.4	NA	2.0 ± 1.1	NA	>100
Complex **6**	<0.1	NA	0.5 ± 0.2	NA	>100
Complex **7**	1.7 ± 0.6	10.6	2.7 ± 0.4	6.7	18.1 ± 5.1
Complex **8**	<0.1	NA	<0.1	NA	16.3 ± 2.1
Complex **9**	<0.1	NA	0.4 ± 0.3	16.5	6.6 ± 1.1
Complex **10**	<0.1	NA	0.9 ± 0.4	3.11	2.8 ± 0.4
Complex **11**	1.4 ± 0.6	68.9	3.6 ± 1.0	26.8	96.5 ± 6.5
Complex **12**	1.9 ± 0.4	52.6	15.4 ± 8.5	NA	>100
Cisplatin	0.9 ± 0.7	43.6	<0.1	392.0	39.2 ± 1.0

*SD (standard deviation of triplicate of two independent experiments).
**SI (selectivity index).

IC_{50} values, calculated from the concentration response curves obtained after 72 h drug treatment employing the MTT test, are shown in table 1. Some compounds presented equal or superior activity when compared to cisplatin.

The free ligands, in B16F10 cell line, did not show any toxicity; however, they were toxic to the CT26.WT cells and showed a high selectivity index in comparison to the normal BHK-21 cell.

Complexes **1–12** were cytotoxic against B16F10 cell while the free ligands were not. Especially for platinum complexes, **2**, **4**, and **6** were 10-fold more potent and 20-fold more selective than the others. All of the palladium complexes showed a high selectivity index. To the CT26.WT cell line, the complex cytotoxicities were very similar to the free ligands. However, platinum compounds **2**, **4**, and **6** and palladium compounds **8**, **9**, and **11** showed a high selectivity index.

The formation of the complexes significantly improved their cytotoxicity in tumor cells, especially for the B16-F10 cell line, without showing toxicity to normal cells (BHK21), improving the selectivity index for most of the complexes.

3.3. *Antibacterial activity*

The antibacterial activities for all complexes were evaluated in six different bacterial strains and compared to chloramphenicol (table S3). Complexes **1** and **7** showed better activity in *S. aureus* (45 and 14 μM, respectively) than chloramphenicol (64 μM) for this strain. The same complexes were also active against *S. dysenteriae* (90 and 54 μM) compared to the same positive control (64 μM). All other compounds did not show antibacterial activity against the tested strains.

Complexes **1** and **7** present the same *R* substituent in the thiosemicarbazone, a benzyl ring, which could be important to establish structure–activity relationships.

4. Conclusion

Potential anticancer Pt(II) and Pd(II) thiosemicarbazone complexes were prepared. The structures of the synthesized complexes were elucidated on the basis of their spectroscopic properties and analytical techniques in addition to quantum mechanical calculations. Theoretical calculations suggest the *trans* configuration of the complexes.

Despite previous reports that many Pd(II) and Pt(II) complexes exhibit antibacterial and antifungal activity [45–47], even complexes with thiosemicarbazones [48, 49], the present compounds did not show significant antibacterial activity.

Nonetheless, the complexes described herein were more cytotoxic than the corresponding free ligands in the tested cell lines, some of them exhibiting activity superior to cisplatin. The development of potential anticancer metal complexes is relevant considering that relatively few of these are in clinical use currently. Platinum complexes are classical antitumor agents and many of them show significant cytotoxicity [50, 51]. On the other hand, although several palladium compounds exhibit antiproliferative properties [52–55], none are approved for commercial distribution yet and it is important to design complexes that are potentially active against cancer.

Acknowledgments

The authors wish to thank CNPq, FAPEMIG and CAPES for financial supports and fellowships. This work is a collaborative research project with members of the Rede Mineira de Química (RQ-MG), supported by FAPEMIG.

References

[1] C.F.J. Barnard, M.J. Cleare, P.C. Hydes. *Chem. Brit.*, **22**, 1001 (1986).
[2] F. Zunino, G. Savi, A. Pasini. *Cancer Chemoth. Pharm.*, **18**, 180 (1986).
[3] A.E. Liberta, D.X. West. *BioMetals*, **5**, 121 (1992).
[4] H. Beraldo, D. Gambino. *Mini-Rev. Med. Chem.*, **4**, 31 (2004).
[5] H. Beraldo. *Quim. Nova*, **27**, 461 (2004).
[6] D. Kovala-Demertzi, M.A. Demertzis, E. Filiou, A.A. Pantazaki, P.N. Yadav, J.R. Miller, Y.F. Zheng, D.A. Kyriakidis. *BioMetals*, **16**, 411 (2003).
[7] L. Feun, M. Modiano, K. Lee, J. Mao, A. Marini, N. Savaraj, P. Plezia, B. Almassian, E. Colacino, J. Fischer, S. MacDonald. *Cancer Chemoth. Pharm.*, **50**, 223 (2002).
[8] N.C. Kasuga, K. Sekino, M. Ishikawa, A. Honda, M. Yokoyama, S. Nakano, N. Shimada, C. Koumo, K. Nomiya. *J. Inorg. Biochem.*, **96**, 298 (2003).
[9] Y. Teitz, D. Ronen, A. Vansover, T. Stematsky, J.L. Riggs. *Antivir. Res.*, **24**, 305 (1994).
[10] N. Karali. *Eur. J. Med. Chem.*, **37**, 909 (2002).
[11] T.S. Lobana, R. Sharma, G. Bawa, S. Khanna. *Coord. Chem. Rev.*, **253**, 977 (2009).
[12] K.O.S. Ferraz, G.M.M. Cardoso, C.M. Bertollo, E.M. Souza-Fagundes, N. Speziali, C.L. Zani, I.C. Mendes, M.A. Gomes, H. Beraldo. *Polyhedron*, **30**, 315 (2011).
[13] Z. Afrasiabi, E. Sinn, S. Padhye, S. Dutta, S. Padhye, C. Newton, C.E. Anson, A.K. Powell. *J. Inorg. Biochem.*, **95**, 306 (2003).
[14] A.G. Quiroga, J.M. Perez, E.I. Montero, D.X. West, C. Alonso, C. Navarro-Ranninger. *J. Inorg. Biochem.*, **75**, 293 (1999).
[15] C.E.P. Goncales, D. Araldi, R.B. Panatieri, J.B.T. Rocha, G. Zeni, C.W. Nogueira. *Life Sci.*, **76**, 2221 (2005).
[16] S.B. Novakovic, G.A. Bogdanovic, V.M. Leovac. *Inorg. Chem. Commun.*, **8**, 9 (2005).
[17] T. Rosu, E. Pahontu, S. Pasculescu, R. Georgescu, N. Stanica, A. Curaj, A. Popescu, M. Leabu. *Eur. J. Med. Chem.*, **45**, 1627 (2010).
[18] T.T. Tavares, G.F. Teixeira, C.M. Lopes, W.T.G. Novato, H. Silva, M.T.P. Lopes, M.V. De Almeida, R.M. Grazul, H.F. Dos Santos, A.P.S. Fontes. *J. Inorg. Biochem.*, **115**, 13 (2012).
[19] H. Silva, A.C.A. Silva, F.O. Lemos, R.L. Monte-Neto, A.P.S. Fontes, M.T.P. Lopes, F. Frezard. *Anti-Cancer Drugs*, **24**, 131 (2013).
[20] L.M.M. Vieira, M.V. de Almeida, H.A. de Abreu, H.A. Duarte, R.M. Grazul, A.P.S. Fontes. *Inorg. Chim. Acta*, **362**, 2060 (2009).
[21] L.M.M. Vieira, M.V. de Almeida, M.C.S. Lourenco, F. Bezerra, A.P.S. Fontes. *Eur. J. Med. Chem.*, **44**, 4107 (2009).
[22] W. Yi, R.H. Cao, Z.Y. Chen, L. Yu, L. Ma, H.C. Song. *Chem. Pharm. Bull.*, **57**, 1273 (2009).
[23] National Committee for Clinical Laboratory Standards (NCCLS), *Performance Standards for Antimicrobial Susceptibility Testing*, Approved standard M100-512, Vol. 22, (2002).
[24] A.D. Becke. *J. Chem. Phys.*, **98**, 5648 (1993).
[25] P.J. Hay, W.R. Wadt. *J. Chem. Phys.*, **82**, 299 (1985).
[26] T.H. Dunning Jr., P.J. Hay. In *Modern Theoretical Chemistry*, H.F. Schaefer III (Ed.), Vol. 3, pp. 1–28, Springer, New York, NY (1976).
[27] D. Paschoal, B.L. Marcial, J.F. Lopes, W.B. De Almeida, H.F. Dos Santos. *J. Comput. Chem.*, **33**, 2292 (2012).
[28] K. Wolinski, J.F. Hilton, P. Pulay. *J. Am. Chem. Soc.*, **112**, 8251 (1990).
[29] G. Scalmani, M.J. Frisch. *J. Chem. Phys.*, **132**, 114110 (2010).
[30] G. Jansen, B.A. Hess. *Phys. Rev. A*, **39**, 6016 (1989).
[31] D. Paschoal and H.F. Dos Santos, in preparation.
[32] M.J. Frisch, G.W. Trucks, H.B. Schlegel, G.E. Scuseria, M.A. Robb, J.R. Cheeseman, G. Scalmani, V. Barone, B. Mennucci, G.A. Petersson, H. Nakatsuji, M. Caricato, X. Li, H.P. Hratchian, A.F. Izmaylov, J. Bloino, G. Zheng, J.L. Sonnenberg, M. Hada, M. Ehara, K. Toyota, R. Fukuda, J. Hasegawa, M. Ishida, T. Nakajima, Y. Honda, O. Kitao, H. Nakai, T. Vreven, J.A. Montgomery, Jr., J.E. Peralta, F. Ogliaro, M. Bearpark, J.J. Heyd, E. Brothers, K.N. Kudin, V.N. Staroverov, R. Kobayashi, J. Normand, K. Raghavachari, A. Rendell, J.C. Burant, S.S. Iyengar, J. Tomasi, M. Cossi, N. Rega, J.M. Millam, M. Klene, J.E. Knox, J.B. Cross, V. Bakken, C. Adamo, J. Jaramillo, R. Gomperts, R.E. Stratmann, O. Yazyev, A.J. Austin, R. Cammi,

C. Pomelli, J.W. Ochterski, R.L. Martin, K. Morokuma, V.G. Zakrzewski, G.A. Voth, P. Salvador, J.J. Dannenberg, S. Dapprich, A.D. Daniels, O. Farkas, J.B. Foresman, J.V. Ortiz, J. Cioslowski, D.J. Fox. *Gaussian 09, Revision A.02*, Gaussian, Inc., Wallingford, CT (2009).
[33] R.P. Tenório, A.J.S. Góes, J.G. de Lima, A.R. de Faria, A.J. Alves, T.M. de Aquino. *Quim. Nova*, **28**, 1030 (2005).
[34] W.S. Hong. *J. Organomet. Chem.*, **689**, 277 (2004).
[35] W. Hernández, J. Paz, A. Vaisberg, E. Spodine, R. Richter, L. Beyer. *Bioinorg. Chem. Appl.*, **2008**, 690952 (2008).
[36] T.S. Lobana, P. Kumari, R.J. Butcher, T. Akitsu, Y. Aritake, J. Perles, F.J. Fernandez, M.C. Vegas. *J. Organomet. Chem.*, **701**, 17 (2012).
[37] J.M. Antelo, L. Adrio, M.T. Pereira, J.M. Ortigueira, J.J. Fernández, J.M. Vila. *Cryst. Growth Des.*, **10**, 700 (2010).
[38] A.H. Al-Kubaisi. *Bull. Korean Chem. Soc.*, **25**, 37 (2004).
[39] I.G. Santos, A. Hagenbach, U. Abram. *Dalton Trans.*, 677 (2004).
[40] A.A. Ali, H. Nimir, C. Aktas, V. Huch, U. Rauch, K.-H. Schafer, M. Veith. *Organometallics*, **31**, 2256 (2012).
[41] H.S. Seleem, A.A. Emara, M. Shebl. *J. Coord. Chem.*, **58**, 1003 (2005).
[42] T.S. Lobana, Rekha, B.S. Sidhu, A. Castineiras, E. Bermejo, T. Nishioka. *J. Coord. Chem.*, **58**, 803 (2005).
[43] M.S. Bakkar, M. Yamin. Siddiqi, M.S. Monshi, *Synth. React. Inorg. Met.-Org. Chem.*, **33**, 1157 (2003).
[44] E. Gabano, E. Marengo, M. Bobba, E. Robotti, C. Cassino, M. Botta, D. Osella. *Coord. Chem. Rev.*, **250**, 2158 (2006).
[45] M.N. Patel, P.A. Dosi, B.S. Bhatt. *J. Coord. Chem.*, **65**, 3833 (2012).
[46] M.A. Carvalho, B.C. Souza, R.E.F. Paiva, F.R.G. Bergamini, A.F. Gomes, F.C. Gozzo, W.R. Lustri, A.L.B. Formiga, G. Rigatto, P.P. Corbi. *J. Coord. Chem.*, **65**, 1700 (2012).
[47] A.C. Moro, A.C. Urbaczek, E.T. de Almeida, F.R. Pavan, C.Q.F. Leite, A.V.G. Netto, A.E. Mauro. *J. Coord. Chem.*, **65**, 1434 (2012).
[48] M. Tyagi, S. Chandra. *Phosphorus*, *Sulfur Silicon Relat. Elem.*, **184**, 778 (2009).
[49] P.I.S. Maia, A. Graminha, F.R. Pavan, C.Q.F. Leite, A.A. Batista, E.S. Lang, J. Ellena, S.S. Lemos, H.S.S. Araújo, V.M. Deflon. *J. Braz. Chem. Soc.*, **21**, 1177 (2010).
[50] C. Gao, F. Fei, T. Wang, B. Yang, S. Gou, J. Yang, L. Liao. *J. Coord. Chem.*, **66**, 1068 (2013).
[51] K.S.O. Ferraz, G.F. Silva, F.M. Costa, B.M. Mendes, B.L. Rodrigues, R.G. dos Santos, H. Beraldo. *BioMetals*, **1**, 10 (2013).
[52] L. Ma, J. Zhang, F. Zhang, C. Chen, L. Li, S. Wang, S. Li. *J. Coord. Chem.*, **65**, 3160 (2012).
[53] J. Zhang, L. Ma, F. Zhang, Z. Zhang, L. Li, S. Wang. *J. Coord. Chem.*, **65**, 239 (2012).
[54] J. Zhang, F. Zhang, L. Wang, J. Du, S. Wang, S. Li. *J. Coord. Chem.*, **65**, 2159 (2012).
[55] K.O.S. Ferraz, G.M.M. Cardoso, C.M. Bertollo, E.M.S. Fagundes, N. Speziali, I.C. Mendes, M.A. Gomes, H. Beraldo. *Polyhedron*, **30**, 315 (2011).